Efficient Geographic Routing over Lossy Links in Wireless Sensor Networks

MARCO ZÚÑIGA ZAMALLOA
University of Southern California
and
KARIM SEADA
Nokia Research Center, Palo Alto
and
BHASKAR KRISHNAMACHARI
University of Southern California
and
AHMED HELMY
University of Florida

Recent experimental studies have shown that wireless links in real sensor networks can be extremely unreliable, deviating to a large extent from the idealized perfect-reception-within-range models used in common network simulation tools. Previously proposed geographic routing protocols commonly employ a maximum-distance greedy forwarding technique that works well in ideal conditions. However, such a forwarding technique performs poorly in realistic conditions as it tends to forward packets on lossy links. Based on a recently developed link loss model, we study the performance of a wide array of forwarding strategies, via analysis, extensive simulations and a set of experiments on motes. We find that the product of the packet reception rate and the distance improvement towards destination ($PRR \times d$) is a highly suitable metric for geographic forwarding in realistic environments.

Categories and Subject Descriptors: C.2.1 [**Computer-Communication Networks**]: Network Architecture and Design—*Wireless Communication*; I.6 [**Simulation and Modeling**]: Simulation Theory—*Systems Theory*

General Terms: Performance, Design, Implementation

Additional Key Words and Phrases: Wireless Sensor Networks, Geographic Routing, Blacklisting

1. INTRODUCTION

Geographic routing is a key paradigm that is quite commonly adopted for information delivery in wireless ad-hoc and sensor networks where the location information of the nodes is available (either *a-priori* or through a self-configuring localization mechanism). Geographic routing protocols are efficient in wireless networks for several reasons. For one, nodes need to know only the location information of their direct neighbors and the final destination in order to forward packets and hence the state stored is minimum. Further, such protocols conserve energy and bandwidth since discovery floods and state propagation are not required beyond a single hop.

The main component of geographic routing is usually a greedy forwarding mechanism whereby each node forwards a packet to the neighbor that is closest to the destination. This can be an efficient, low-overhead method of data delivery if it is reasonable to assume (i) sufficient network density, (ii) reasonably accurate localization and (iii) high link reliability independent of distance within the physical radio range.

However, while assuming highly dense sensor deployment and reasonably accurate localization may be acceptable in some classes of applications, it is now clear that assumption (iii) pertaining to the ideal disk model (in which there are perfect links within a given communication range, and none beyond) is unlikely to be valid in any realistic deployment. Several recent experimental studies on wireless ad-hoc and sensor networks [De Couto et al. 2005; Ganesan et al. 2003; Woo et al. 2003; Zhao and Govindan 2003] have shown that wireless links can be highly unreliable and that this must be explicitly taken into account when evaluating the performance of higher-layer protocols. Figure 1 (a) shows samples from a statistical link layer model developed in [Zuniga and Krishnamachari 2004] — it shows the existence of a large "transitional region" where the link quality has high variance, including both good and highly unreliable links.

The existence of such unreliable links exposes a key weakness in greedy forwarding that we refer to as the *weakest link* problem. At each step in greedy forwarding, the neighbors that are closest to the destination (also likely to be farthest from the forwarding node) may have poor links with the current node. These "weak links" would result in a high rate of packet drops, resulting in drastic reduction of delivery rate or increased energy wastage if retransmissions are employed. Figure 1 (b) illustrates the striking discrepancy between the performance of greedy forwarding on the realistic lossy network versus a network with an idealized reception model.

This observation brings to the fore the concept of neighbor classification based on link reliability. Some neighbors may be more favorable to choose than others, not only based on distance, but also based on loss characteristics. This suggests that a *blacklisting/neighbor selection* scheme may be needed to avoid 'weak links'. But, what is the most energy-efficient forwarding strategy and how does such strategy draw the line between 'weak' and 'good' links?

We articulate the following energy trade-off between distance per hop and the overall hop count, which we simply refer to as the *distance-hop energy trade-off* for geographic forwarding. If the geographic forwarding scheme attempts to minimize the number of hops by maximizing the geographic distance covered at each hop (as in greedy forwarding), it is likely to incur significant energy expenditure due
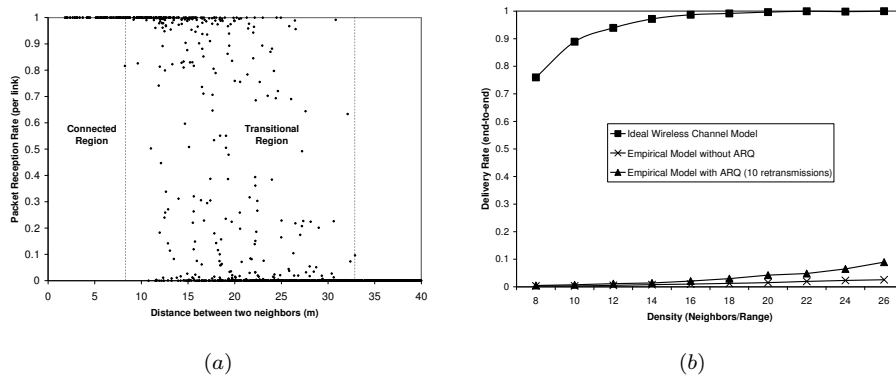
Fig. 1. (a) Samples from a realistic analytical link loss model (b) An illustration of the discrepancy of performance of greedy geographic forwarding between an idealized perfect-reception model and the lossy reception model

to retransmission on the unreliable long weak links. On the other hand, if the forwarding mechanism attempts to maximize per-hop reliability by forwarding only to close neighbors with good links, it may cover only a small geographic distance at each hop, which would also result in greater energy expenditure due to the need for more transmission hops for each packet to reach the destination. We will show in this paper that the optimal forwarding choice is generally to neighbors in the transitional region.

In this work, our goal is to study the energy and reliability trade-offs pertaining to geographic forwarding in depth, both analytically and through extensive simulations, under a realistic packet loss model. For this reason, we utilize the statistical packet loss model derived in [Zuniga and Krishnamachari 2004]. We emphasize, however, that the framework, fundamental results and conclusions of this paper are quite robust and not limited by the specific characteristics of this model. The main contributions of this work include:

—Mathematical analysis of optimal forwarding choices to balance the distance-hop energy trade-off for both ARQ and No-ARQ scenarios.

—Introduction of several blacklisting/link-selection strategies based on distance, PRR and a combination of both, and a framework to evaluate them in the context of geographic routing. The framework is applicable for various channel models, even though we apply it in this study to a specific set of channel parameters.

—The conclusion that PRR×distance is an optimal metric for making localized geographic forwarding decisions in lossy wireless networks with ARQ mechanisms. We also find that a best reception-based strategy shows close performance.

—Validation of this conclusion using a set of experiments with motes to compare basic geographic forwarding approaches.

Before proceeding we present the scope of our work. This study focuses on those classes of sensor networks in which the flow is low-rate, the schedule of reporting is non-overlapping, or non-CSMA MAC is used such that MAC collisions

are at minimum (or non-existent). This a reasonable characteristic of many low-rate/time-scheduled applications such as habitat monitoring [Szewczyk et al. 2004]. Investigation of MAC collisions in high-rate sensor networks is outside the scope of this paper and is subject to future work.

The rest of the paper is organized as follows. The related work is described in section 2. In section 3, we present the statistical link-loss model, scope and metrics of our work. Then, we provide a mathematical analysis of the optimum distance in the presence of unreliable links in section 4. A set of tunable geographic forwarding strategies is presented in section 5, and in section 7, we evaluate the performance of these strategies. The effectiveness of the PRR×distance metric is validated through experiments with motes in section 8. Finally, we discuss the implications of our results in section 9.

2. RELATED WORK

Our study is informed by prior work on geographic forwarding and routing, as well as recent work on understanding realistic channel conditions and their impact on wireless network routing protocols.

Early work in geographic routing considered only greedy forwarding [Finn 1987] by using the locations of nodes to move the packet closer to the destination at each hop. Greedy forwarding fails when reaching a local maximum, a node that has no neighbors closer to the destination. A number of papers in the past few years have presented face/perimeter routing techniques to complement and enhance greedy forwarding [Bose et al. 2001; Karp and Kung 2000; Kuhn et al. 2003]. More details about geographic and position-based routing schemes can be found in the following surveys [Mauve et al. 2001; Seada and Helmy 2005].

On the other hand, much of the prior research done in wireless ad hoc and sensor networks, including geographic routing protocols, has been based on a set of simplifying idealized assumptions about the wireless channel characteristics, such as perfect coverage within a circular radio range. It is becoming clearer now to researchers and practitioners that wireless network protocols that perform well in simulations using these assumptions may actually fail in reality.

Several researchers have pointed out how simple radio models (e.g., the ideal binary model assumption that there are perfect links between pairs of nodes within a given communication range, beyond which there is no link) may lead to wrong results in wireless ad hoc and sensor networks. Ganesan *et al.* [Ganesan et al. 2003] present empirical results from flooding in a dense sensor network and study different effects at the link, MAC, and application layers. They found that the flooding tree exhibits a high clustering behavior, in contrast to the more uniformly distributed tree obtained with the ideal model. Kotz *et al.* [Kotz et al. 2003] enumerate the set of common assumptions used in MANET research, and provide data demonstrating that these assumptions are not usually correct. The real connectivity graph can be much different from the ideal disk graph, and losses due to fading and obstacles are common at a wide range of distances and keep varying over time. The communication area covered by the radio is neither circular nor convex, and is often noncontiguous.

Zhao and Govindan [Zhao and Govindan 2003] report measurements of packet

delivery for a dense sensor network in different indoor and outdoor environments. Their measurements also point to a gray area within the communication range of a node, where there is large variability in packet reception over space and time. Similarly, the measurements obtained by the SCALE connectivity assessment tool [Cerpa et al. 2003] show that there is no clear correlation between packet delivery and distance in an area of more than 50% of the communication range (which corresponds to the transitional region we consider in our work).

Several recent studies have shown the need to revisit routing protocol design in the light of realistic wireless channel models. In [De Couto et al. 2005], De Couto *et al.* have measurements for DSDV and DSR, over a 29 node 802.11b test-bed and show that the minimum hop-count metric has poor performance, since it is not taking the channel characteristics into account especially with the fact that minimizing the hop count maximizes the distance traveled by each hop, which is likely to increase the loss ratio. They present the expected transmission count metric that finds high throughput paths by incorporating the effects of link loss ratios, asymmetry, and interference. Draves *et al.* [Draves et al. 2004] extended the study of the ETX metric by comparing it with other metrics: per-hop round trip time and per-hop packet pair. Based on a wireless test-bed running a DSR-based routing protocol, they confirmed that the ETX metric has the best performance when all nodes are stationary.

On the same line of work, Woo *et al.* [Woo et al. 2003] study the effect of link connectivity on distance-vector based routing in sensor networks. They too identify the existence of the three distinct reception regions: connected, transitional, and the disconnected regions. They evaluate link estimator, neighborhood table management, and reliable routing protocols techniques. A frequency-based neighbor management algorithm (somewhat related to the blacklisting techniques studied in our work) is used to retain a large fraction of the best neighbors in a small-size table. They show that cost-based routing using a minimum expected transmission metric shows good performance. The concept of neighbor management via blacklisting of weak links is also found in the most recent versions of the Directed Diffusion Filter Architecture and Network Routing API [Silva et al. 2003]. More recently in [Zhou et al. 2006], empirical data is used to study the impact of radio irregularity in sensor networks. The results show that radio irregularity has more significant impact on routing protocols than on MAC protocols and that location-based protocols perform worse in the presence of radio irregularity than on-demand protocols.

On the other hand, there is a vast literature in the wireless communication area proposing techniques to exploit spatial and temporal diversity to improve the gain of the wireless channel. Rake receivers [Bottomley et al. 2000; Liu and Li 1999] combat multi-path fading by using several "sub-receivers". Each receiver has a slight delay to tune the individual multi-path components, and each component is decoded independently and combined at a later stage to increase the signal-to-noise ratio of the received signal. Multiple input multiple output (MIMO) techniques [Foschini 1996; Chuah et al. 2002] use cooperative systems to exploit multi-path propagation to increase data throughput and range. While the techniques described above are purely physical layer approaches, recently some studies have explored the interac-

tion between cooperative diversity techniques, in the physical layer, and routing, in the network layer. In [Chen et al. 2005], the authors consider in a unified fashion the effects of cooperative communication via transmission diversity and multi-hopping as well as optimal power allocation schemes in fading channels. Khandani *et. al.* [Khandani 2004] use omni-directional antennas to optimize the energy efficiency on the transmission of a single message from a source to destination through sets of nodes acting as cooperating relays. Our work differs from the previous in that it uses only techniques at the network layer based on inexpensive radios that do not require any extra functionality at the physical layer.

This work is a revised and more thorough study than our original work [Seada et al. 2004]. Some of the contributions of this extended version are:

—Analysis of the impact of different channel, radio and deployment parameters on the optimal forwarding distance and on the relative performance of different forwarding strategies with respect to PRR×d

—Quantify the difference between our local optimal metric PRR×d and the global optimal ETX.

—Showing the impact of the different strategies when face routing is used to overcome greedy disconnections. (In [Seada et al. 2004] we had assumed that only greedy forwarding is allowed).

Our initial work sparked the interest in the community on optimal geographic forwarding strategies on lossy links, and some works have followed-up on our initial study. In [Lee et al. 2005], the authors propose a new metric called *normalized advance* (NADV), which also studies the *distance-hop trade-off* and provides some flexibility in terms of the metric to be optimized, such as energy or delay.

In [Zhang et al.], the $PRR \times d$ is studied, among other metrics, for 802.11b networks. It is suggested in this work that link quality (in the context of their particular 802.11-based network) should be tested using using on-the-fly data traffic rather than through periodic beacons. We should clarify that the $PRR \times d$ metric itself is agnostic to how the packet reception rate is measured. We note that for highly dynamic environments where link qualities fluctuate rapidly so that it is not possible to obtain valid, stable PRR estimates, our scheme may not be suitable. However, our work is suitable for a large class of sensor networks, where the sensors are static and the environment is relatively stable to get estimates of PRR. Some recent work on modeling temporal variations of link quality [Cerpa et al. 2005] may be useful in extending our work to dynamic conditions.

Although the minimum expected transmission metric (ETX) used in [De Couto et al. 2005] and [Woo et al. 2003] is somewhat related to our $PRR \times d$ metric in trying to reduce the total number of transmissions from source to destination and thus minimize the energy consumed, the minimum expected transmission metric is a global path metric, while $PRR \times d$ is a local link metric suitable for scalable routing protocols such as geographic routing. We shall compare the $PRR \times d$ metric with the global metric in this work.

Li *et al.* [Li et al. 2005] study an extension of this work that is suitable for environments where nodes can vary the power level. A modified version of the $PRR \times d$ metric that incorporates the power usage is proposed in that work.
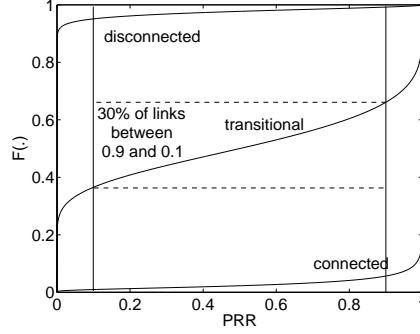
Fig. 2.   *cdf*s for packet reception rate for receivers in different regions.

3.   MODEL, SCOPE, ASSUMPTIONS AND METRICS

Model: For both the analysis and simulations undertaken in this study, we required a realistic link layer model for sensor networks. The selected model is the one derived in [Zuniga and Krishnamachari 2004], which is based on the log-normal path loss model [Rappaport 2002][1]. In the next paragraphs we present a brief description of that link layer model.

According to the log normal path loss model the received power (P_r) at a distance d is a random variable in dB given by:

$$P_r(d) = P_t - PL(d_0) - 10 \ \eta \ log_{10}(\frac{d}{d_0}) + \mathcal{N}(0, \sigma) \tag{1}$$

Where P_t is the output power, η is the path loss exponent (rate at which signal decays with respect to distance), $\mathcal{N}(0, \sigma)$ is a Gaussian random variable with mean 0 and variance σ^2 (due to multi-path effects), and $PL(d_0)$ is the power decay for the reference distance d_0.

For a transmitter-receiver distance d, the signal-to-noise ratio (Υ_d) at the receiver is also a random variable in dB, and it can be derived from equation (1):

$$\begin{aligned} \Upsilon_d &= P_r(d) - P_n \\ &= P_t - PL(d_0) - 10\eta \ log_{10}(\frac{d}{d_0}) + \mathcal{N}(0, \sigma) - P_n \\ &= \mathcal{N}(\mu(d), \sigma) \end{aligned} \tag{2}$$

Where $\mu(d)$ is given by:

$$\mu(d) = P_t - PL(d_0) - 10 \ \eta \ log_{10}(\frac{d}{d_0}) - P_n \tag{3}$$

---

[1]While the log-normal path loss model has been mostly known for modeling shadowing in medium and large coverage systems, in [Rappaport 2002] and [Seidel and Rappaport], the model is proposed for small coverage systems (where transmitter-receiver distances are in the order of meters). Furthermore, empirical studies have shown that the log-normal path loss model provides more accurate multi-path channel models than Nakagami and Rayleigh for small-scale indoor environments [Nikookar and Hashemi 1993]

The values of the signal-to-noise ratio from equation (2) can be inserted on any of the available bit-error-rate (BER) expressions available in the communication literature. In this paper we assume the BER expression corresponding to non-coherent frequency shift keying (NC-FSK) radios, however, the results and insights are valid for any narrow-band radio. NC-FSK radios were chosen because the empirical evaluation in section 8 uses this type of radios. The packet reception rate (PRR) for NC-FSK radios and a transmitter-receiver distance d is a random variable given by:

$$\Psi_d = \Psi(\Upsilon_d) = \left(1 - \frac{1}{2}\exp^{-10^{\frac{\Upsilon_d}{10}}\frac{1}{1.28}}\right)^{\rho \times 8f} \quad (4)$$

Where ρ is the encoding ratio (2 for Manchester encoding), f is the frame length in bytes, and γ is the signal to noise ratio in dB (an instance of the random variable defined in equation (2)). Figure 1 (a) shows an instance of the link layer derived from equation (4), which resembles the behavior of empirical studies [Zhao and Govindan 2003; Woo et al. 2003].

In this work, we will also use some of the expressions derived in the link layer model presented in [Zuniga and Krishnamachari 2004] and [Marco Zú and Krishnamachari 2007]. Among them are (a) the beginning and end of the transitional region, (b) the expectation of the packet reception rate as a function of distance and (c) the cumulative distribution function of the packet reception rate. The next paragraphs describe briefly these expressions.

Even though there are no strict definitions for the beginning and end of the different transmission regions in the literature, one valid definition is the following:

Definition 1: In the connected region links have a high probability ($> p_h$) of having high packet reception rates ($> \psi_h$).

Definition 2: In the disconnected region links have a high probability ($> p_\ell$) of having low packet reception rates ($< \psi_\ell$).

The transitional region is the region between the end of the connected region and the beginning of the disconnected region; and p_h and p_ℓ can be chosen as any numbers close to 1 and 0 respectively. The expressions for the beginning (d_s) and end (d_e) of the transitional region are given by:

$$d_s = 10^{\frac{P_n + \gamma_h - P_t + PL(d_0) + 2\sigma}{-10n}}$$
$$d_e = 10^{\frac{P_n + \gamma_\ell - P_t + PL(d_0) - 2\sigma}{-10n}} \quad (5)$$

Where γ_h and γ_ℓ are the SNR values in dB corresponding to ψ_h and ψ_ℓ, respectively. In this paper, we consider the same values used in [Zuniga and Krishnamachari 2004] to define the size of the different regions: $\psi_h = 0.9$, $\psi_\ell = 0.1$, $p_h = 0.96$ and $p_\ell = 0.04$.

In general, the packet reception rate in wireless links is not monotonically decreasing with distance, however, the expected value of the packet reception rate is monotonically decreasing with distance, and it is given by:

$$E[\Psi_d] = \int_{-\infty}^{\infty} \Psi_d(\gamma)f(\gamma)\ \delta\gamma \tag{6}$$

In [Marco Zú and Krishnamachari 2007], the authors introduce the following expression for the cumulative distribution *cdf* of the packet reception rate:

$$F(\psi) = 1 - Q\left(\frac{\Psi^{-1}(\psi) - \mu(d)}{\sigma}\right) \tag{7}$$

Where ψ is an specific value of the PRR in the interval (0,1), $\Psi^{-1}(\psi)$ is the inverse function of equation (4), $\mu(d)$ is given in equation (3) and Q is the tail integral of a unit Gaussian ($Q - function$).

Figure 2 shows an example of the cumulative distribution $F(\Psi)$ for three different transmitter-receiver distances: end of connected region, middle of transitional region and beginning of disconnected region. This figure shows a trend that will be central in understanding the performance of the different forwarding strategies analyzed in this work (sections 6 and 7). Independent of the region where the receiver is, the link has a higher probability of being above 0.9 or below 0.1 (either a good or bad link) than being between 0.9 and 0.1. For instance, in the middle of the transitional region a link has a 70% probability of being above 0.9 or below 0.1; and at the connected and disconnected regions the probability is even higher ($\sim 95\%$).

It is important to remark that the model considers several channel parameters (η, σ) and radio characteristics (f, ρ). The particular expression shown in equation (4) resembles a mica2 mote, which uses non-coherent frequency shift keying as the modulation technique and Manchester as the encoding scheme (ρ=2).

Scope: Our work presents techniques to reduce the energy consumption of geographic routing during communication events (transmission and reception of packets). Nevertheless, we should offer some caveats regarding the scope of our work. Our models do not consider other means of energy savings such as sleep/awake cycles, transmission power control[2], nor other sources of energy consumption such as processing or sensing. This study focuses on low-rate/time-scheduled applications such as habitat monitoring [Szewczyk et al. 2004], where interference is at minimum (or non-existent). Interference is an important characteristic to consider, specially in medium and heavy traffic scenarios, and is subject to future work.

Assumptions: Our analysis and simulations are based on the following assumptions:

—Nodes know the location and the link quality (PRR) of their neighbors.

—Nodes know the position of the final destination

—A link (neighbor) is considered valid if its packet reception rate is higher than a non-zero threshold ψ_{th}.

Even though the definition of a valid link presented in this work (last bullet point) may be too generous and it would not suit practical purposes[3], we present

---

[2]Li *et al.* present an interesting extension of our work in [Li et al. 2005], which includes power control.

[3]In real deployments links below 10% or 30% may not be considered as valid links

a set of blacklisting strategies that performs some filtering on link quality before using them for routing purposes. Hence, we purposely set loose restrictions on the definition of a valid wireless link in order to evaluate the entire spectrum.

Metrics: From the end-user perspective, an efficient sensor network should provide as much data as possible utilizing as little energy as possible. Hence, in order to evaluate the energy efficiency of different strategies we use the following metrics:

—Delivery Rate (r): percentage of packets sent by the source that reach the sink.
—Total Number of Transmissions (t): total number of packets sent by the network to attain delivery rate r.
—Energy Efficiency (ξ): number of packets delivered to the sink for each unit of energy spent by the network in communication events.

The goal of an optimal forwarding strategy is to maximize ξ, which can be derived from the delivery rate r and the total number of transmissions t. Let p_{src} be the number of packets sent by the source, e_{tx} and e_{rx} the amount of energy required by a node to transmit and receive a packet. Therefore, the total amount of energy consumed by the network for each transmitted packet is given by:

$$e_{\text{total}} = e_{\text{tx}} + e_{\text{rx}} \tag{8}$$

Hence, the total energy due to communication events is $t \times e_{\text{total}}$, and ξ is given by:

$$\xi = \frac{p_{\text{src}}\, r}{e_{\text{total}}\, t} \quad \rightarrow \quad \xi \ \propto \ \frac{r}{t} \tag{9}$$

Where p_{src} and e_{total} are constants, t is a random variable, and r could be a constant or a random variable depending if the system is using automatic repeat request or not, as explained in the next section. Table I presents the notation used in this work.

4. ANALYTICAL MODEL

Given a realistic link layer model, akin to the one described in section 3, *our goal is to explore the distance-hop trade-off in order to maximize the energy efficiency of the network during communication events.*

4.1 Problem Description

This sub-section describes the notation and set-up used in the analysis. We assume that nodes are placed every τ meters in a chain topology[4]. A nominal transmission range of $2\lfloor d_e \rfloor$ is considered, where d_e is the end of the transitional region (equation (5)), the set of distances to the neighbors is given by $\varphi = \{\tau, 2\tau, 3\tau, ..., 2\lfloor d_e \rfloor\}$[5], and the distance between source and sink is denoted by $d_{\text{src}-\text{sink}}$.

---

[4]A non-constant distance between nodes can be also chosen. However, a constant distant τ allows a fair comparison of the different regions (connected, transitional, disconnected)
[5]The selection of $2\lfloor d_e \rfloor$ as a "nominal range" does not affect the results of this work. Even though other distances can be considered, $2\lfloor d_e \rfloor\tau$ was selected because it can derived from equation (6) that nodes beyond this distance have a small probability of having valid links.

Description	Symbol
Packet Reception Rate Parameters	
- packet reception rate (PRR) [Random Process]	Ψ
- packet reception rate for a distance d [Random Variable]	Ψ_d
- cumulative distribution function of Ψ_d	$F(\psi)$
- expected packet reception rate	$E[\Psi]$
- an instance of R.V. Ψ_d	ψ
- blacklisting threshold	ψ_{th}
Signal to Noise Ratio Parameters	
- signal to noise ratio (SNR)	Υ
- an instance of R.V. Υ_d	γ
- SNR value corresponding to ψ_{th}	γ_{th}
Channel Parameters	
- path loss exponent	η
- standard deviation	σ
- output power	P_t
Transitional Region Parameters	
- end of transitional region	d_e
Energy Efficiency Parameters	
- end-to-end delivery rate	r
- end-to-end number of transmissions	t
- energy efficiency	ξ
- energy spent by network for one transmission	e_{total}
- optimal forwarding distance	d_{opt}
- distance between source and sink	$d_{\text{src}-\text{snk}}$
- number of packets transmitted by source	p_{src}
- number of hops	h
- set of distances to neighbors	φ

Table I.   Mathematical Notation

Let ξ_d be the random variable that denotes the energy efficiency obtained if a distance d is traversed at each hop, then, the optimal forwarding distance d_{opt} is the one that maximizes the expected value of ξ_d:

$$d_{\text{opt}} = \arg \max_{d \in \varphi} E[\xi_d] \tag{10}$$

In the next subsections we derive optimal local forwarding metrics for the ARQ and No-ARQ cases.

4.2   Analysis for ARQ case

We assume no *a-priori* constraint on the maximum number of retransmissions (i.e. ∞ retransmissions can be performed), therefore, r is equal to 1, and according to equation (9) the energy efficiency is given by:

$$\xi_{\text{ARQ}} = \frac{p_{\text{src}}}{e_{\text{total}}\, t} \tag{11}$$

Letting Ψ_d be the random variable representing the PRR for a transmitter-receiver distance d, the expected number of transmissions at each hop is $\frac{p_{\text{src}}}{\Psi_d}$. The
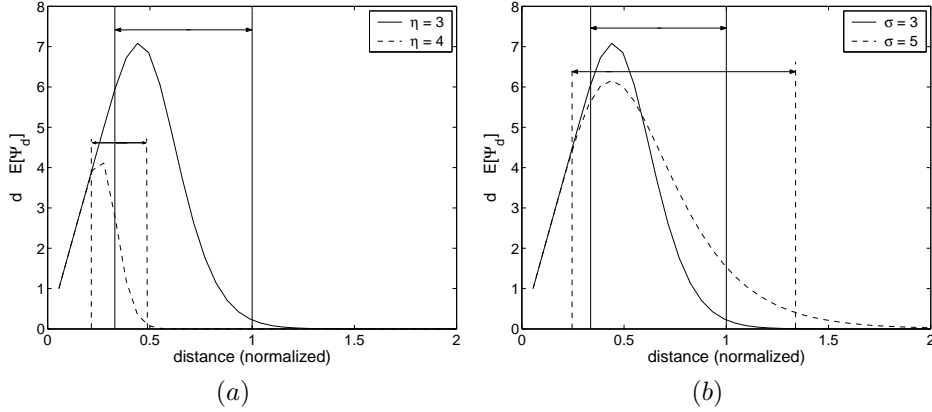
Fig. 3. Impact of channel multi-path on $E[\xi_{d_{ARQ}}]$, (a) impact of path loss exponent η, (b) impact of channel variance σ.

number of hops h is equal to $\frac{d_{\text{src}-\text{sink}}}{d}$, therefore, the total number of transmission t is given by:

$$t = \frac{d_{\text{src}-\text{sink}}}{d}\frac{p_{\text{src}}}{\Psi_d} \tag{12}$$

Substituting t in equation (11), we obtain the energy efficiency metric for a transmitter-receiver distance d:

$$\xi_{d_{ARQ}} = \frac{d\Psi_d}{e_{\text{total}}d_{\text{src}-\text{sink}}} \tag{13}$$

d is defined (constant) for Ψ_d, therefore, the expected value of $\xi_{d_{ARQ}}$ is given by:

$$E[\xi_{d_{ARQ}}] = \frac{dE[\Psi_d]}{e_{\text{total}}d_{\text{src}-\text{sink}}} \tag{14}$$

e_{total} and $d_{\text{src}-\text{sink}}$ are constants and an expression for $E[\Psi_d]$ was presented in equation (6). Hence, in order to maximize the energy efficiency of systems with ARQ we need to maximize $dE[\Psi_d]$ (PRR$\times$distance product).

The computation of $E[\Psi_d]$ involves the Q function (tail-integral of the Gaussian distribution) for which no closed-form expressions are known. Hence, we evaluate equation (10) numerically for all $d \in \varphi$.

Figures 5 (a) and (b) depict the impact of the path loss exponent η and log-normal variance σ on $d \times E[\xi_{d_{ARQ}}]$, respectively. In both figures, the black curve represents an scenario with the following parameters: τ=1m, η=3, σ=3, P_t=-10 dBm and f=100; and the x-axis represent the transmitter-receiver distance d normalized with respect to the end of the transitional region, which is approximately 20 meters for the parameters given above. The beginning and end of the transitional region are depicted by vertical lines, and it is interesting to observe that the distance d with the highest energy efficiency is in the transitional region.
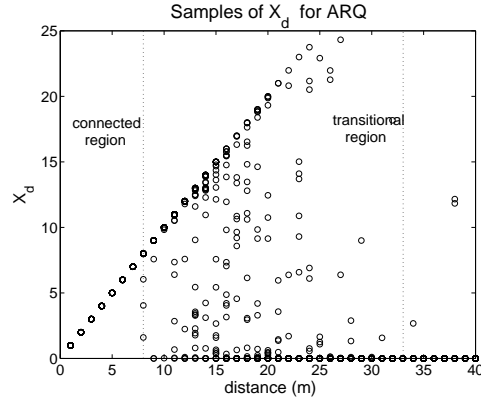
Fig. 4. Energy efficiency metric for the ARQ case. The transitional region often has links with good performance as per this metric.

Figure 5 (a) presents the impact of the path loss exponent η. We observe that for a higher η the optimal forwarding distance shifts left. This is due to the fact that for a higher path loss exponent the received signal strength decays faster, which in turn reduces the expected packet reception rate, nevertheless, the forwarding distance with the highest energy efficiency is still within the limits of the transitional region (vertical dotted lines). Figure 5 (b) presents the impact of the channel variance σ. In this case the forwarding distances close to the end of the transitional region increase their energy efficiency, while the distances close to the beginning of the transitional region decrease their efficiency. This is due to the fact that a higher σ increases the probability of finding good links farther away from the sender, but also decreases the probability of finding good links close to the sender. It is important to highlight that while the beginning and end of the transitional region also change due to σ (as shown by the vertical dotted lines), the optimal forwarding distance still lies within it. The appearance of the optimal forwarding distance within the transitional region for all the cases presented in Figure 5 confirms the distance-hop trade-off that geographic routing faces in real deployments.

In actual deployments, the packet reception rate takes an instance of the r.v. Ψ_d, hence, the optimal local forwarding metric for a node is the one that maximizes the product of the PRR of the link and the distance to the neighbor (PRR×d). Figure 4 shows simulations for the PRR×d metric in a line topology, where for each neighbor, the PRR obtained was multiplied by its distance. It can be observed that nodes in the transitional region usually have the highest value for this metric.

4.3   Analysis for the No-ARQ case

In systems with ARQ, at each step a node transmits the same amount of data as the source ($r = 1$), this characteristic allowed us to do the analysis independently of $d_{\mathrm{src-sink}}$. On the other hand, in systems without ARQ the amount of data decreases at each hop, hence in order to maintain an acceptable delivery rate, the longer the $d_{\mathrm{src-sink}}$ the higher the PRR of the chosen links should be. The analysis in this section explains this behavior.

Letting $i \in [1, 2, ..., \lceil h \rceil]$ be the hop counter, we denote Ψ_d^i as the r.v. representing the packet reception rate for the distance d traversed at each hop i. Ψ_d^i are $i.i.d$ $\forall i \in [1, 2, ..., \lceil h \rceil]$. This notation allow us to define the delivery rate r for systems without ARQ traversing a distance d at each hop:

$$r = p_{\mathrm{src}} \prod_{i=1}^{\lceil h \rceil} \Psi_d^i \tag{15}$$

The number of packet transmissions required at each hop i (t^i) is given by:

$$t^i = p_{\mathrm{src}} \prod_{j=1}^{i} \Psi_d^{(j-1)} \tag{16}$$

Where $\Psi_d^0 = 1$, to accommodate for the number of transmissions required at the source (equal to p_{src}). The total number of transmissions t is the sum of t_i, $\forall i \in [1, 2, ..., \lceil h \rceil]]$. Therefore, t is given by:

$$t = p_{\mathrm{src}} \sum_{i=1}^{\lceil h \rceil} \left(\prod_{j=1}^{i} \Psi_d^{(j-1)} \right) \tag{17}$$

Then $\xi_{d_{\mathrm{woARQ}}}$ is given by:

$$\xi_{d_{\mathrm{woARQ}}} = \frac{\displaystyle\prod_{i=1}^{\lceil h \rceil} \Psi_d^i}{\displaystyle\sum_{i=1}^{\lceil h \rceil} \left(\prod_{j=1}^{i} \Psi_d^{(j-1)} \right)} \tag{18}$$

In actual deployments, each link will take an instance of the random variable. Letting ψ be an instance of the PRR for a given link, at each hop the local calculation of the delivery rate would be $r = p_{\mathrm{src}} \psi^{\lceil h \rceil}$ and the number of transmissions would be sum given by:

$$t = p_{\mathrm{src}} \sum_{i=1}^{\lceil h \rceil} \psi^{(i-1)} = p_{\mathrm{src}} \frac{(\psi)^h - 1}{\psi - 1)} \tag{19}$$

Which leads to the following forwarding metric:

$$Metric_{\mathrm{woARQ}} = \frac{(\psi)^h(\psi-1)}{e_{\mathrm{total}}((\psi)^h-1)} = \frac{(\psi)^h(1-\psi)}{e_{\mathrm{total}}(1-(\psi)^h)} \tag{20}$$

Given that the PRR of a link is in the interval (0,1), $\frac{(1-\psi)}{1-(\psi)^h} < 1$, and for large number of hops, $(\psi)^h$ in the numerator decreases exponentially while $1 - (\psi)^h$ in the denominator increases. Therefore, equation (20) shows that in systems without ARQ, specially for large number of hops, nodes should choose links with high PRRs. Otherwise for long distances the delivery rate and the energy efficiency will tend to zero.

5. GEOGRAPHIC FORWARDING STRATEGIES FOR LOSSY NETWORKS

In this section, we present some forwarding strategies that will be compared with the PRR×d metric. The aim of these strategies is to avoid the *weakest link problem*, and they are classified into two categories: distance-based and reception-based. In distance-based policies nodes need to know only the distance to their neighbors, while in reception-based policies, in addition to the distance, nodes need to know also the link's PRR of their neighbors. All the strategies use greedy-like forwarding, in that first a set of neighbors is blacklisted based on a certain criteria and then the packet is forwarded to the node closest to the destination among the remaining neighbors.

5.1 Distance-based Forwarding

Original Greedy: Original greedy is similar to the current forwarding policy used in common geographic routing protocols. Original greedy is a special case of the coming blacklisting policies, when no nodes are blacklisted.

   Distance-based Blacklisting: In this case, each node blacklists neighbors that are above a certain distance from itself. In this work the "nominal" radio range is defined as $2d_e$. For example if the radio range is considered to be 40 m and the blacklisting threshold is 20%, then the farthest 20% of the radio range (8 m) is blacklisted and the packet is forwarded through the neighbor closest to the destination from those neighbors within 32 m.

5.2 Reception-based Forwarding

Absolute Reception-based Blacklisting: In absolute reception-based blacklisting, each node blacklists neighbors that have a reception rate below a certain threshold. For example, if the blacklisting threshold is 20%, then only neighbors closer to the destination with a reception rate above 20% are considered for forwarding the packet.

   Best Reception Neighbor: Each node forwards to the neighbor that has the highest PRR and is closer to the destination. This strategy is ideal for systems without ARQ.

5.3 PRR×d

This is the metric shown in our analysis and it can be observed as a mixture of the distance (d) and reception (PRR) based. For each neighbor, that is closer to the destination, the product of the PRR and distance is computed, and the neighbor with the highest value is chosen.

6. COMPARISON OF DIFFERENT STRATEGIES

The model derived in section 4 provides the optimal forwarding distance. Nevertheless, in order to accurately evaluate the distance-hop trade-off we need to quantify *the amount of energy saved by choosing the best candidate according to the optimal metric with respect to other methods.* In this section, we compare analytically the energy efficiency of the different strategies presented in the previous section for systems with ARQ in a chain topology.

   In order to compare the different strategies we require their expected energy

efficiency ($E[\xi]$). In general, a strategy S has an expected energy efficiency $E[\xi_S]$ given by:

$$E[\xi_S] = \sum_{d \in \varphi} E[\xi_S | d_f = d] \; p(d_f = d)$$
$$= \sum_{d \in \varphi} E[\xi_S | d_f = d] \; q_d \quad (21)$$

Where φ is the set of distances to neighbors, d_f is the distance traveled at each hop, and q_d is the probability that $\xi_d > \xi_\ell, \forall \ell \in \varphi, \ell \neq d$. In the remainder of this section we denote the conditioned random variable $\xi_{\mathrm{d}} = \{\xi | d_f = d\}$. The next subsections provide $E[\xi]$ for different strategies.

6.1 PRR×d

For the PRR×d metric, q_d is given by:

$$q_d = \int_0^\infty P((x < \xi_d < x + dx) \wedge (\xi_j < x, \forall j \in \varphi, j \neq d)) \; dx \quad (22)$$

The energy efficiency of different distances can be considered independent [6]:

$$q_d = \int_0^\infty P(x < \xi_d < x + dx) \; P(\xi_j < x, \forall j \in \varphi, j \neq d) \; dx \quad (23)$$

Finally, q_d given by:

$$q_d = \int_0^\infty f_{\xi_d}(x) \prod_{\forall j \in \varphi, j \neq d} F_{\xi_j}(x) \; dx \quad (24)$$

Where $f_{\xi_d}(x)$ and $F_{\xi_d}(x)$ are the *pdf* and *cdf* of the metric ξ_d. Given that these density functions depend on the Q function we provide numerical solutions in Figure 5 for q_d. This figure shows the impact of different parameters on q_d.

Figures 5 (a) and (b) show that when τ and η increase the probability q_d shifts left, closer to the connected region. On the other hand, when σ and P_t increase q_d shifts right, closer to the end of the transitional region. These behavior is explained by the change in the number of neighbors (node density with respect to the coverage range).

The higher the number of neighbors, the higher the probability of discovering neighbors with good links (high PRR) that are closer to the destination (longer distances), which increases q_d. Keeping all the parameters constants, a larger τ or a higher η (faster signal decay) reduces the density. On the other hand, a higher P_t increases the coverage range, and higher σ increases the probability of finding good links farther away from the sender. Hence, the higher the density (number of neighbors), the higher q_d.

---

[6]The link quality (PRR) is a function of the SNR which is the sum of many contributions, coming from different locations [Rappaport 2002].

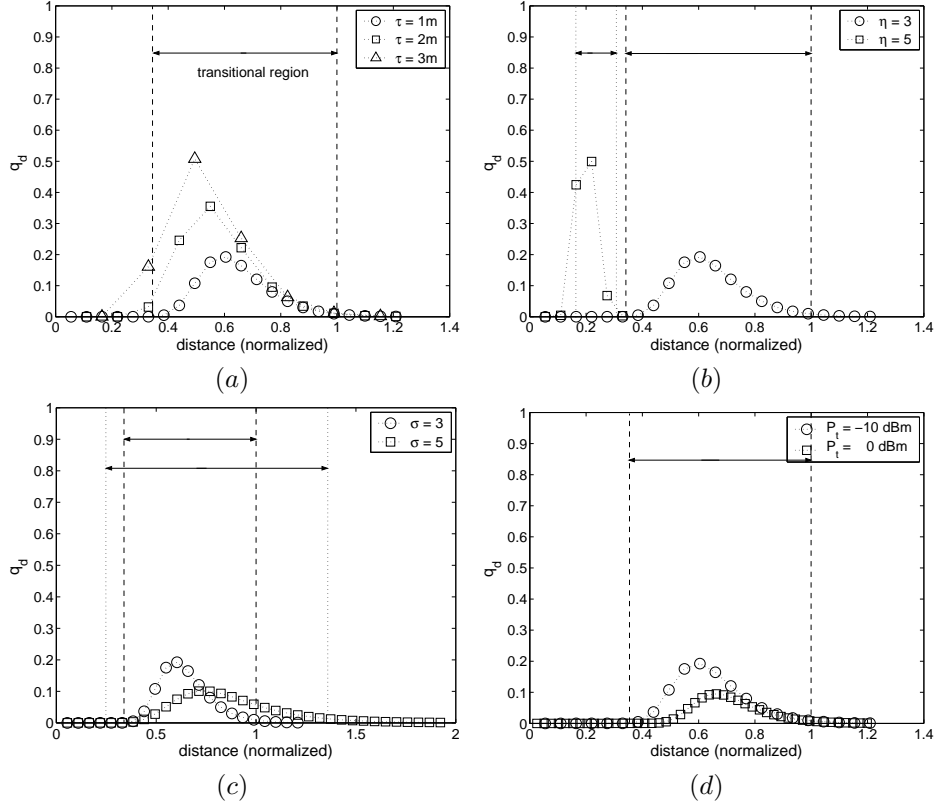Fig. 5. Impact of different parameters on q_d for the PRR×d metric, (a) τ, (b) η, (c) σ, (d) P_t

The expected energy efficiency of the packet reception rate for a distance d is given by equation (14). Hence, according to equation (21) the expected energy efficiency for systems with ARQ using the PRR×d metric is given by:

$$E[\xi_{\text{PRR}\times\text{d}}] = \sum_{d\in\varphi} \frac{dE[\Psi_d]}{e_{\text{total}}d_{\text{src}-\text{sink}}} q_d \qquad (25)$$

6.2 Absolute Reception-Based

Let us define ψ_{th} as the blacklisting threshold of absolute reception, which implies that valid links have PRR values on the interval $[\psi_{th}, 1)$. In order to choose d as the forwarding distance, links with distances longer than d should have a PRR $< \psi_{th}$, and the link at distance d should have a PRR $\geq \psi_{th}$. Hence, q_d for absolute reception-based (ARB) blacklisting is given by:

$$q_{d_{\text{ABR}}} = p(\Psi_d \geq \psi_{th}) \prod_{\text{d}_{\text{w}}\in\varphi,\text{d}_{\text{w}}>\text{d}} p(\Psi_{d_w} < \psi_{th}) \qquad (26)$$

Given that a link is considered valid if $\Psi_d \geq \psi_{th}$, the expected number of transmissions at each hop is $\frac{p_{\text{src}}}{E[\Psi_d|\Psi_d > \psi_{th}]}$. Hence, the expected value of the energy efficiency conditioned on the fact that $\Psi_d > \psi_{th}$ is given by:

$$E[\xi_{d_{\text{ARB}}}] = \frac{d}{e_{\text{total}}\, d_{\text{src-snk}}} E[\Psi_d|\Psi_d > \psi_{th}] \tag{27}$$

Denoting $\gamma = \Psi^{-1}(\psi)$ and $\gamma_{th} = \Psi^{-1}(\psi_{th})$ the probability density function of the packet reception rate conditioned on $\Psi_d > \psi_{th}$ is $f(\psi|\Psi_d > \psi_{th})$, which can be mapped to SNR values as $f(\gamma|\Upsilon_d > \gamma_{th})$, then:

$$\begin{aligned} E[\Psi_d|\Psi_d > \psi_{th}] &= \int_{\psi_{th}}^{1} \psi f(\psi|\Psi_d > \psi_{th})d\psi \\ &= \int_{-\gamma_{th}}^{+\infty} \Psi(\gamma)f(\gamma|\Upsilon_d > \gamma_{th})d\gamma \end{aligned} \tag{28}$$

Combining the previous two equations we obtain the expected energy efficiency for absolute reception base (ARB):

$$E[\xi_{\text{ARB}}] = \sum_{d\in\varphi} \frac{dE[\Psi_d|\Psi_d > \psi_{th}]}{e_{\text{total}}\, d_{\text{src-snk}}} q_{d_{\text{ABR}}} \tag{29}$$

6.3 Distance-Based

When the blacklisting is based on distance the energy efficiency of the forwarding distance d (ξ_d) is the same as equation (14). Denoting d_{th} as the distance blacklisting threshold, distance based blacklisting will select a distance d the neighbor at distance d has a PRR>0 and the neighbors with distances longer than d have a PRR=0. The probability q_d of distance based (DB) blacklisting is given by:

$$q_{d_{\text{DB}}} = p(\Psi_d > 0) \prod_{d_{\text{w}}\in\varphi, d < d_{\text{w}} < d_{\text{th}}} p(\Psi_{d_w} = 0) \tag{30}$$

Finally, the expected energy efficiency is given by:

$$E[\xi_{\text{DB}}] = \sum_{d\in\varphi, d\leq d_{\text{th}}} \frac{dE[\Psi_d]}{e_{\text{total}} d_{\text{src-sink}}} q_{d_{\text{DB}}} \tag{31}$$

6.4 Comparison

Figures 6 and 7 show the comparison of energy efficiency for distance based and reception based blacklisting strategies. These figures show the impact of different channel, radio and deployment parameters. The figures show the relative performance of the different strategies with respect to the PRR×d metric, i.e. the y axis show the how much extra energy is required to attain the same delivery rate as PRR×d. Similarly to section 4, the base model of comparison have parameters τ=1, η=3, σ=3, P_t=-10 dBm and f=100. Original greedy is a specific case of distance-based blacklisting, when no distance is blacklisted; and best reception
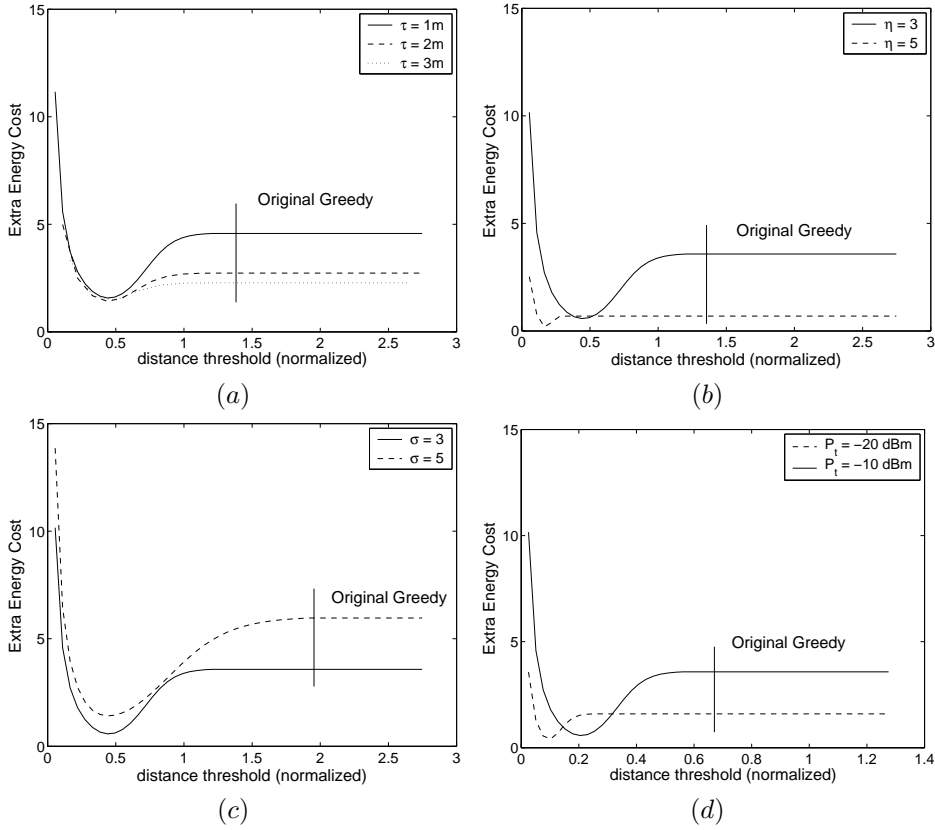
Fig. 6.   Performance of Distance Based blacklisting

is a specific case of absolute reception-based when a high blacklisting threshold is selected.

Figure 6 confirms the significant energy expenditure of original greedy, but there are other important insights from these comparisons. First, both figures (6 and 7) show that τ, η, σ and P_t have an important impact on the relative performance of the different metrics due to its influence in the number of neighbors (node density per coverage range) and the expected energy efficiency. An increase in τ or η, or a decrease in P_t leads to a lower node density, which implies that the strategies will start to choose the same nodes, given the lack of options, and the energy efficiency will be more similar among them. When σ is increased, it improves the performance of absolute reception-based and decreases the one of distance-based. This is due to the fact that σ increases the probability of both, encountering good links at farther distances and bad links at shorter distances. Second, Figure 7 shows that blacklisting links with PRR below 1% improves significantly the performance of reception-based. This is due to the observation done in section 3 (Figure 2) with respect to the *cdf* of the PRR, where it was noted that most of the links are either "good" or "bad", hence, by blacklisting links below 1% a significant fraction
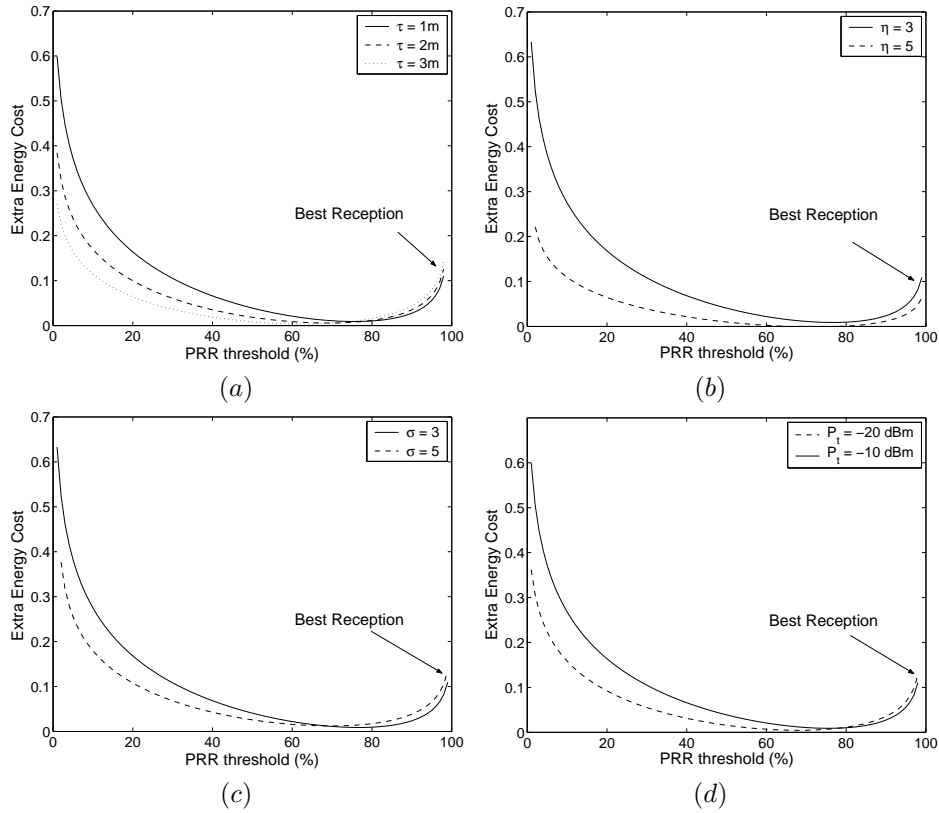
Fig. 7.   Performance of Reception Based blacklisting

of the remaining links are good. Third, reception-based strategies perform better than distance-based. This due to the fact that reception-base takes advantage of good quality links in the transitional region (farther away from the transmitter), on the other hand, distance-based blacklist potential good links, furthermore, the closer the distance does not necessarily imply better links, and distance-based is still vulnerable to select bad-quality links at medium distances. Fourth, it is important to consider that while some thresholds of distance and absolute reception based strategies show close performance to that of PRR×dist, these values change according to the channel, radio and deployment parameters requiring a pre-analysis of the scenario, on the other hand, PRR×d is a local metric that does not require any *a priori* configuration. Finally, the results show that Best Reception is also a good metric and it can be good candidate for systems without ARQ given that these systems require to select good quality links.

7.   SIMULATION

In the previous section the analysis restricted to an ideal chain topology where the risk of disconnection was not considered. In real scenarios, network connectivity, specially at low densities, can have a significant impact on the performance of geo-

graphic routing protocols. In this section, we perform extensive simulations to test the performance of the proposed forwarding schemes in more realistic environments with different densities and network sizes.

In the simulations, nodes are deployed uniformly at random, and for each pair of nodes we use equation (4) to generate the packet reception rate of the link. Also on this section we add a new blacklisting strategy – on top of the ones presented in section 5. This new strategy is called Relative Reception Based Blacklisting

In relative reception-based blacklisting, a node blacklists an specific percentage of neighbors that have low reception rate. For example, if the blacklisting threshold is 20%, it considers only the 80% highest reception rate neighbors of its neighbors that are closer to the destination. Note that relative blacklisting is also different from the previous blacklisting methods in that the neighbors blacklisted are different for every destination. Relative blacklisting has the advantage of avoiding the disconnections that can happen in previous methods where all neighbors could be blacklisted, on the other hand, it also risks having bad neighbors that may be wasteful to consider.

We simulate random static networks of sizes ranging from 100 to 1000 nodes having the same radio characteristics. The density is presented as the average number of nodes per a nominal radio range and vary it over a wide scale: 25, 50, 100, 200 nodes/range. Recall that in our work, the nominal range is set to $2\lfloor d_e \rfloor$, which is 40 m for the parameters used in this section. Even though the densities may seem high, in real scenarios nodes within a distance range are not necessary detected as neighbors, hence, the number of *detected* neighbors can be significantly less; the simulations consider a node as a neighbor if its PRR is at least 1%.

In each simulation run, nodes are placed at random locations in the topology. Among these nodes, a random source and a random destination are chosen[7]. 100 packet transmissions are issued from source to destination and there are no concurrent flow transmissions. The results are computed as the average of 100 runs.

During packet transmission, the packet header contains the destination location and each node chooses the next hop based on the routing policy used. If the packet is dropped, the response depends on whether ARQ is used or not. If ARQ is not used, this packet is lost; if ARQ is used, we consider two cases when the packet is retransmitted indefinitely (∞) or for a maximum of 10 retransmissions. Since the minimum reception rate for a node considered as a neighbor is 1%, infinite retransmissions are guaranteed to succeed.

The performance metrics studied are the delivery rate, the total number of transmissions, and the energy efficiency (bits/unit energy) as defined in Section 3. Several parameters for the different forwarding strategies were tested, however due to space restrictions, we present here only some of the key results.

In the coming subsections we compare the different strategies by first selecting the optimum blacklisting threshold for distance and absolute reception based for each density. Then, these optimized threshold-based strategies are compared with original greedy, best reception policy, and the best PRR×d policy. After that,

---

[7]These characteristics are common on wireless sensor networks with mobile users, where events are considered to occur with equal probability at any node, and the mobile user can select any of the nearby nodes as the sink.
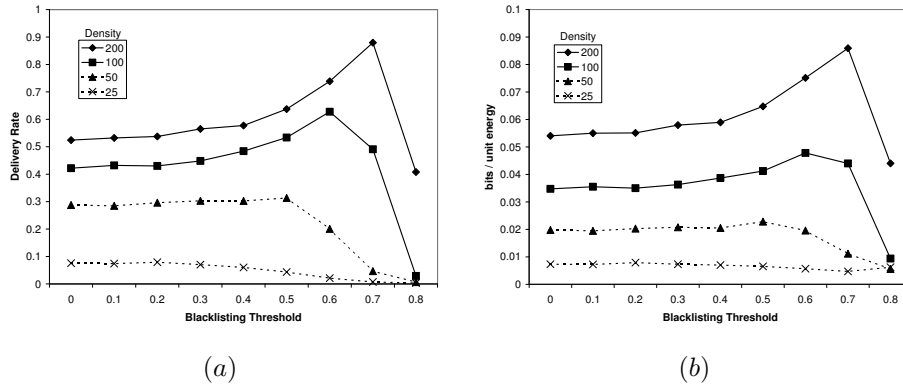
Fig. 8. Performance of Distance-based Blacklisting Schemes for Geographic Forwarding: (a) Delivery Rate, (b) Energy Efficiency
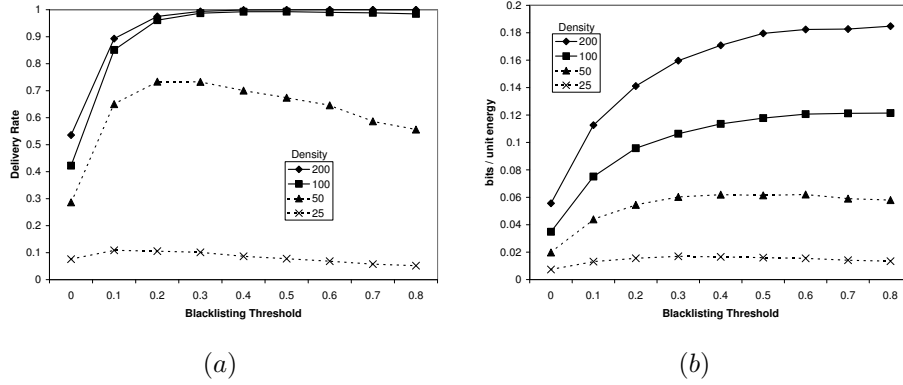

Fig. 9. Performance of Absolute Reception-based Blacklisting Schemes for Geographic Forwarding: (a) Delivery Rate, (b) Energy Efficiency

we present results for various distance ranges between source-destination pairs and compare the different policies at these ranges. We will present also some insights on the effects of ARQ and network size on the policies, and an evaluation for how our local optimum strategy compares to the global optimum expected transmission count (ETX). Finally, we will include face routing in the evaluation and discuss its results.

7.1   Comparison of Forwarding Strategies

In order to make a fair comparison we first need to obtain the optimum blacklisting thresholds for distance and absolute reception for all densities. We use networks of 1000 nodes and set the number of ARQ retransmissions to 10.

Figures 8 (a) and (b) show the delivery rate and energy efficiency for distance-based blacklisting. The optimum blacklisting thresholds are within the transitional
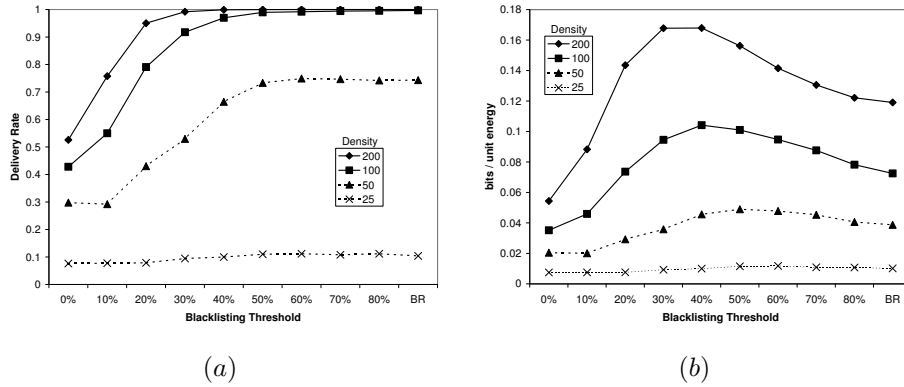
Fig. 10. Performance of Relative Reception-based Blacklisting Schemes for Geographic Forwarding: (a) Delivery Rate, (b) Energy Efficiency
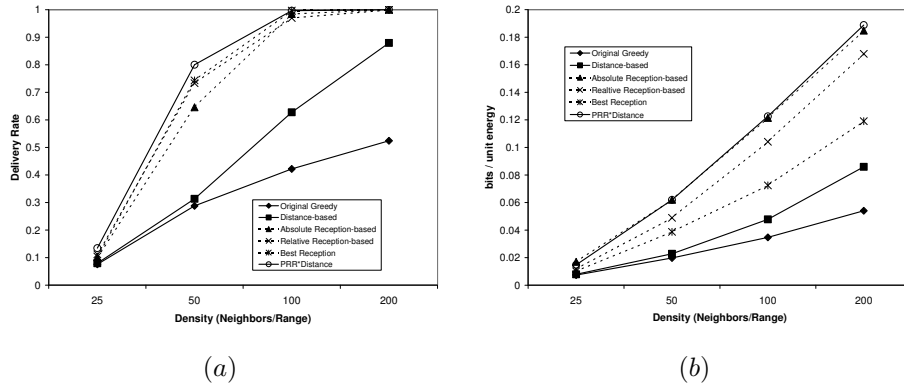

Fig. 11. Performance of Geographic Forwarding Strategies at Different Densities: (a) Delivery Rate, (b) Energy Efficiency

region which conforms with our analysis. The delivery rate is low at low thresholds, because packets can encounter low quality links; at high thresholds, the delivery rate decreases again due to greedy disconnections, when all nodes closer to the destination are blacklisted. The blacklisting threshold has a trade-off between the quality of the link, the number of hops and the greedy connectivity. Also, as the density gets lower, the optimum threshold shifts to the left, since at lower densities the possibility of greedy disconnections is higher. The energy efficiency ξ decreases at higher thresholds because of the larger number of hops required (*distance-hop energy trade-off*), and due to the wasted overhead of transmitting packets over multiple hops before being dropped due to greedy disconnections. It is also important to notice that at low densities, increasing the threshold does not cause much improvement, which indicates that distance-based policies are not ideal for low-dense scenarios.
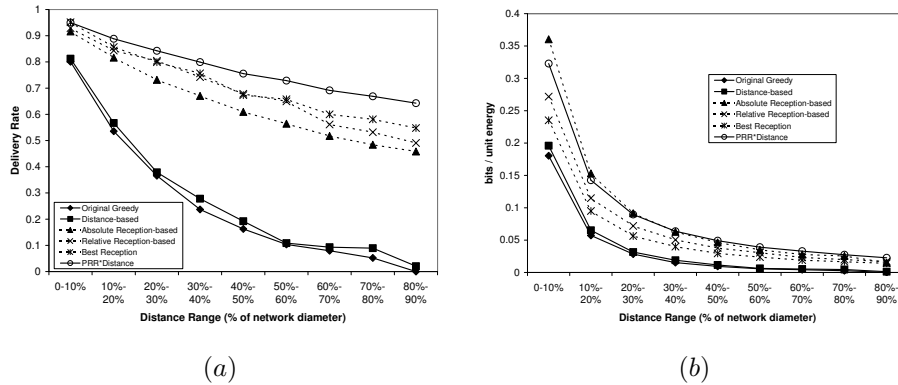
Fig. 12. Performance of Geographic Forwarding Strategies at Different Source-Destination Distances. Each 10% distance range corresponds to about 1.5 times the nominal radio range (40 m): (a) Delivery Rate, (b) Energy Efficiency

Figures 9 (a) and (b) show the delivery rate and energy efficiency for absolute reception-based blacklisting. Compared to distance-based strategies, reception-based policies provide in general higher delivery rates and energy efficiency. A sharp increase in delivery rate happens at 10% threshold since most of the bad links are blacklisted (Figure 2), and 10 retransmissions on average are adequate to deliver the packet[8]. At higher densities (100 and 200), higher thresholds increase the delivery rate and energy efficiency since more and better links are available and the possibility of disconnections is low. While at lower densities (25, 50), high thresholds may create greedy disconnections and impact negatively the delivery rate and energy efficiency.

In Figures 10 (a) and (b) we show the performance for relative reception-based blacklisting. Best Reception (BR in the x-axis) is included as an extreme of relative blacklisting. The main merit of relative blacklisting is that it reduces disconnections by using the best available links independent of their quality or distance; on the other hand, sometimes this causes bad links to be used which reduces the energy efficiency. We notice that at all densities, higher thresholds improve the delivery rate since better links are used with lower risk of increasing the greedy disconnections. However, the energy efficiency has its highset values for intermediate thresholds. When threshold is increased from small to intermediate values better links are used which reduces the retransmission overhead, but at high thresholds the good-quality links are also likely to be close to the forwarding node, which increases the number of hops (*distance-hop energy trade-off*). This behavior also indicates that choosing the node with the best reception rate is not the most energy efficient approach in systems with ARQ.

We should note that the threshold values of different blacklisting methods are not comparable, since they lead to different number of neighbors, link qualities, and neighbor distances. We note also that the optimum thresholds and in general the

---

[8]In general, the reception-based threshold should be lower than the number of retransmissions.

optimum strategies with regard to energy efficiency may not provide the desired delivery rate and may not be satisfactory to provide the required connectivity.

Figures 11 (a) and (b) compare the performance of the optimized threshold strategies with original greedy, best reception and PRR×d for networks of 1000 nodes and 10 retransmissions (ARQ). The delivery rate is low at low densities because of greedy failures. PRR×distance has the highest delivery rate, followed by best reception, relative reception-based, absolute reception-based, distance-based, and finally original greedy. The relative strategies (PRR×distance, best reception, and relative reception-based) have the highest delivery rate, because they reduce greedy disconnections, and strategies based on reception rate are better than those based only on distance. PRR×distance and absolute reception-based blacklisting are the most energy efficient, followed by relative reception-based, best reception, distance-based, and finally original greedy. Also, as predicted in section 6, higher densities lead to bigger differences in performance.

In the previous results we have shown the average performance in delivering packets between random source-destination pairs. Since, the performance may depend on the traffic pattern and the distances between the expected sources and destinations, we study here the effect by the source-destination distance. Figure 12 shows the results for different distance ranges for a density of 50 nodes/range. The delivery rate and the energy efficiency decrease as the distance range increase, since more hops (more transmissions) are required and the probability of packet drops and greedy disconnections become higher. The order of the forwarding strategies remains the same as in the previous comparison.

The comparisons in this subsection show that PRR×d is a very effective strategy conforming with our analysis. It is mostly the highest for both delivery rate and energy efficiency. PRR×d is also easier to implement, since no scenario-dependent absolute threshold parameter is required. Best reception has a high delivery rate, but its energy efficiency is relatively lower due to the *distance-hop energy trade-off*. Conversely, absolute reception-based has a relatively high energy efficiency, since it avoids wasting overhead on links with low reception rates, but its delivery rate is lower due to greedy disconnections.

7.2   Effects of ARQ and Network Size

In this subsection, we study the impact of the network size on ARQ by comparing the performance of original greedy and PRR×d for three systems: ARQ with 10 retransmissions, ARQ with infinite retransmissions and systems without ARQ. The density for all network sizes is 50 nodes/range.

Figure 13 shows that the delivery rate of original greedy increases significantly by using more retransmissions, which confirms the *weakest-link* problem (forwarding through low quality links). On the other hand, the energy efficiency of original greedy degrades with more retransmissions, due to the extra overhead of retransmitting on bad links, which shows that dealing with bad links by just using more retransmissions may improve the delivery rate, but at a cost of a very high energy and bandwidth wastage.

In Figure 14, the delivery rate of PRR×d improves from systems without ARQ to ARQ with 10 retransmission, but there is no significant gain by allowing an unbounded number of retransmissions. This behavior is due to the fact that PRR×d
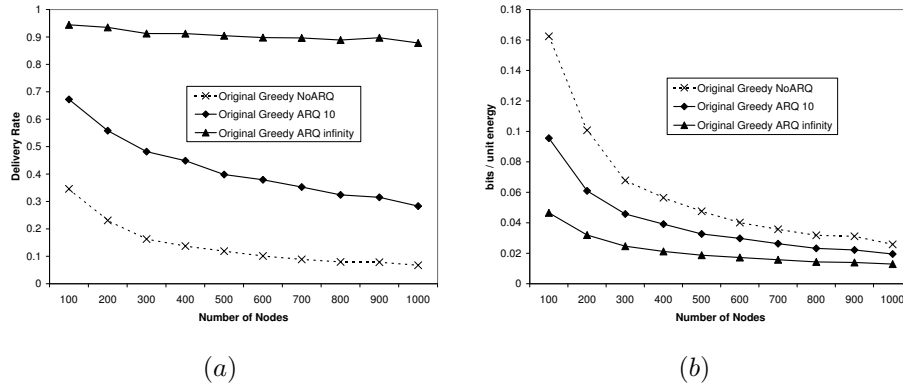
Fig. 13. Performance of Original Greedy with and without ARQ at Different Network Sizes: (a) Delivery Rate, (b) Energy Efficiency
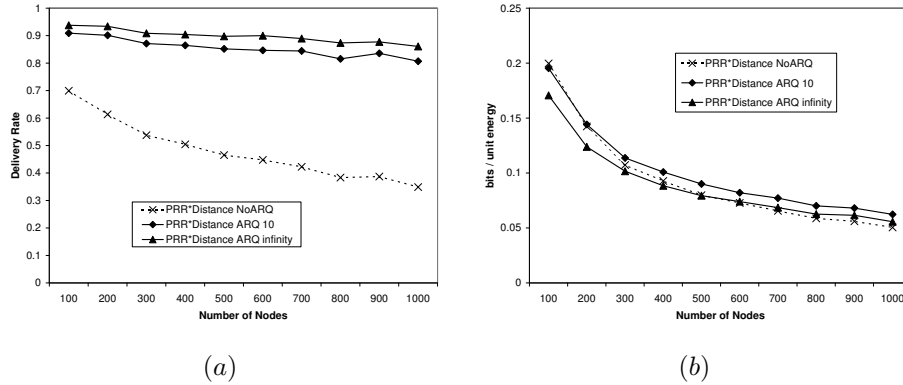

Fig. 14. Performance of PRR×distance with and without ARQ at Different Network Sizes: (a) Delivery Rate, (b) Energy Efficiency

includes the quality of the link in its metric, and thus tend to avoid weak links. The energy efficiency of ARQ with 10 retransmissions is the highest, since it has a high delivery rate (slightly lower than infinite ARQ) and its overhead is limited. We notice that ARQ becomes more efficient as we increase the network size, which is also indicated by our analysis. The reason is that without ARQ the delivery rate reduces due to a higher of dropping the packet over several hops, and in addition, there is extra wasted overhead due to delivering packets over hops before being dropped.

7.3   Comparison to Global ETX

The PRR×d metric is an local optimal greedy metric which minimizes the expected number of transmissions. Other works [De Couto et al. 2005; Woo et al. 2003] have studied global optimal strategies to minimize the expected number of
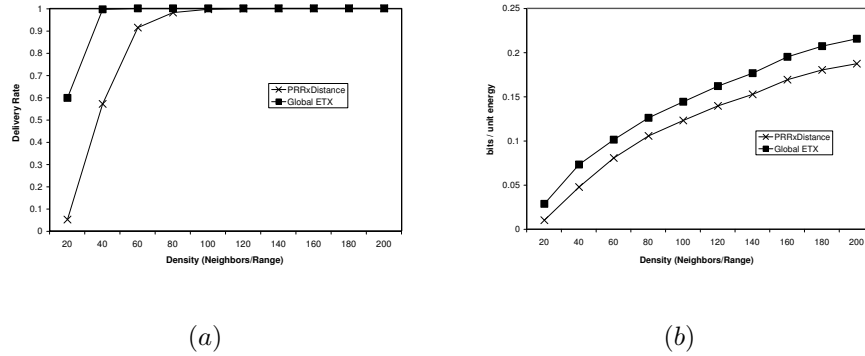
Fig. 15. Performance of $PRR \times d$ compared to Global ETX at Different Densities: (a) Delivery Rate, (b) Energy Efficiency
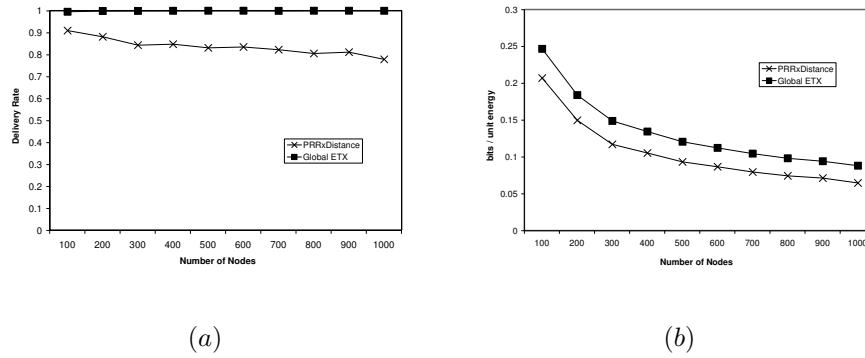

Fig. 16. Performance of $PRR \times d$ compared to Global ETX at Different Network Sizes: (a) Delivery Rate, (b) Energy Efficiency

transmissions (ETX), which chooses the path with the minimum expected number of transmissions based on global information.

In geographic routing, nodes use only local information about their direct neighbors, and hence, optimal local metrics such as PRR×d are ideal. However, it is important to evaluate the difference in performance between local and global metrics. In this section we compare PRR×d with ETX for different network sizes and densities. For ETX, we use Dijkstra algorithm to compute the shortest path from the source to the destination, where the weight of each link is equal to the reciprocal of its PRR.

Figure 15 shows the delivery rate and energy efficiency of PRR×d and ETX at different densities in networks of 1000 nodes. And Figure 16 shows the delivery rate and energy efficiency at a fixed density (50 neighbors/range) and different network sizes.

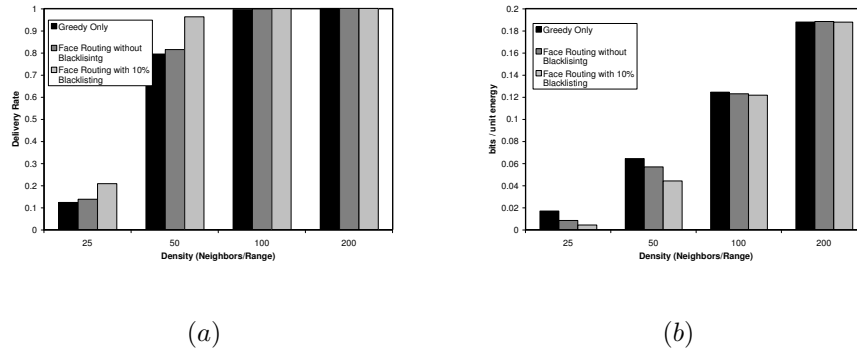(a)   (b)

Fig. 17. Comparison between Greedy forwarding, face routing without blacklisting and face routing with blacklisting: (a) Delivery Rate, (b) Energy Efficiency

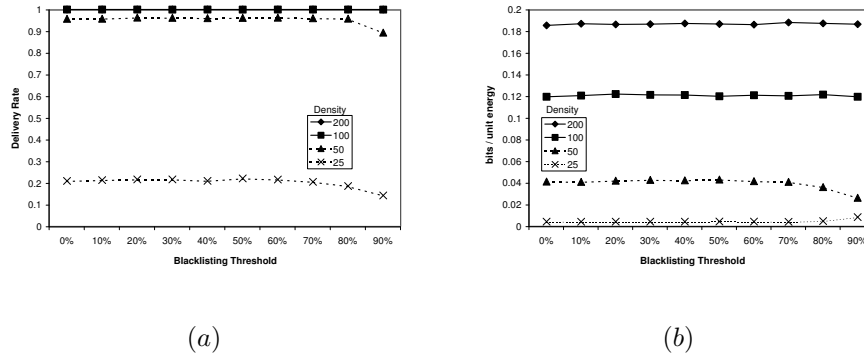(a)   (b)

Fig. 18. Face routing with relative $PRR \times d$ blacklisting at different thresholds: (a) Delivery Rate, (b) Energy Efficiency

The delivery rate is perfect at high densities (Figure 15 (a)), but at low densities the delivery rate of PRR×d is lower, since it is not guaranteed to find a path to the destination, if one exists. Also, the delivery rate of PRR×d decreases at larger networks (Figure 16 (a)), since paths become longer and the probability of path disconnections increases.

An interesting observation is that the energy performance for different densities and network sizes is similar (Figure 15 (b) and Figure 16 (b)). We believe that this narrow difference is due to the spatial locality of the graph. The transmission coverage is limited by a geographical area, and hence, no significant improvement is obtained by requesting link connectivity information from nodes that are far away because there are no links with these nodes.

7.4   Face Routing

To complete our study of geographic routing, in this section we look at face routing under the realistic wireless channel model. Face routing is used when greedy forwarding cannot make any more progress toward the destination. Greedy forwarding stops when the packet reaches a node that has no neighbor closer to the destination or when all the retransmissions fail. In this section, we use greedy forwarding with the PRR×d metric.

Face routing is used on a planar embedding of the graph (using GG planarization) until reaching a node closer to the destination. We have examined different blacklisting strategies for face routing: distance-based blacklisting, reception-based blacklisting, relative reception-based blacklisting, and relative PRRxd. We simulated networks of 1000 nodes at different densities: 25, 50, 100, 200 nodes/range. And ARQ with 10 retransmissions is used at the link layer.

Figure 17 (a) and (b) are showing a comparison of the delivery rate and energy efficiency between greedy forwarding only, face routing without any blacklisting and face routing with blacklisting nodes having a PRR below 10%. The main observations in our results are the following:

- Face routing without any blacklisting does not have significant improvement on delivery rate. A simple blacklisting mechanism that blacklists the very bad links (we blacklist all links below 10% given that the number of retransmissions is 10) has a more significant improvement.

- Although the delivery rate improves with face routing, at low densities the energy efficiency decreases as the delivery rate increases. We suppose that the reason for that is due to long face traversals. With blacklisting, the graphs get also sparser and longer faces are traversed. In general, the overhead of face routing is higher than greedy forwarding so that for each extra percentage of delivery achieved by face routing a significant amount of overhead is consumed.

- More complex blacklisting mechanisms and higher blacklisting thresholds do not have any noticeable variation in delivery rate and energy efficiency from the simple mechanism. We evaluated the 4 mentioned blacklisting strategies at different thresholds and the performance were the same at reasonable thresholds, as long as we are avoiding the very weak links and avoiding very high thresholds that magnify disconnections. For example, Figure 18 is showing the delivery rate and energy efficiency of face routing using a percentage of the links with the highest $PRR \times d$ among the links having a PRR above 10%.

In the results, we are not including the overhead of generating the planar or semi-planar graph itself. For local planarization algorithms like GG and RNG the computations are local based on location information obtained from beacons. To deal with location inaccuracies, additional algorithms may be used. If a localized algorithm is used, such as the mutual witness in [Seada et al. 2004], then the extra overhead may be negligible/ minimal. However, if a non-local planarization algorithm like CLDP [Kim et al. 2005] is used, extra overhead will be generated that will depend on the frequency of network changes and the need to repeatedly run the planarization algorithm. We are not expecting that the face routing performance trend itself will be much affected by the specific planarization algorithm used as long as a graph is generated for face routing.

The performance of geographic routing in our scenarios is largely dependent on greedy forwarding, since it is the main used component. This is more noticed in higher density networks. Other than avoiding the very weak links, variations in face routing blacklisting mechanisms does not affect overall geographic routing performance.

8. EXPERIMENTS WITH MOTES

In order to validate our methodology and conclusions, we undertook an experimental study on motes. Twenty-one (21) mica2 motes were deployed in a chain topology spaced every 60 cm ($\sim$2 feet). The source (node 0) and sink (node 20) were placed at opposite extremes of the chain. The power level was set to -20 dBm and the frame size was 50 bytes. Three different forwarding strategies were tested:

—OG: neighbor closer to the sink whose PRR$>$0.

—BR: neighbor with highest PRR. In case two or more neighbors have the same PRR, the one closer to the sink is chosen.

—PRR$\times$d: neighbors are classified according to the PRR$\times$d metric.

First, the motes exchange test packets to measure the PRR of the links and populate their routing tables accordingly. Afterwards, the source sends 50 packets to the sink for each of the 3 different strategies (150 total). A maximum of 5 transmissions (1 transmission + 4 retransmissions) are allowed at each hop, if the packet is not received after the fifth attempt, it is dropped.

Six different scenarios are studied: a football field, an indoor-building environment and four different outdoor-urban areas. The channel characteristics of some scenarios are significantly different, and hence, instead of providing a cumulative result, we present the results for each one of them.

Table II shows the delivery rate (r), the number of transmission (t), and the energy efficiency (ξ) for the different scenarios. BR have an r of 100% in all scenarios, and PRR$\times$d have 100% for all scenarios except scenario-4 (82%). Greedy performs poorly in most of them with zero or close to zero r in most cases.

r (%)	sce1	sce2	sce3	sce4	sce5	sce6
OG	0	2	32	0	0	94
BR	100	100	100	100	100	100
PRR$\times$d	100	100	100	82	100	100
t	sce1	sce2	sce3	sce4	sce5	sce6
OG	70	110	312	78	121	858
BR	652	407	730	754	701	903
PRR$\times$d	563	425	632	547	560	883
Relative ξ (%)	sce1	sce2	sce3	sce4	sce5	sce6
OG	inf	inf	+54	inf	inf	+3
BR	+16	-4	+16	+14	+25	+2
PRR$\times$d	0.0	0.0	0.0	0.0	0.0	0.0

Table II. Empirical Results for Different Forwarding Strategies. Notice that the relative ξ of PRR$\times$DIST is 0.0 since it is used as the basis of comparison.

With regard to the number of transmissions, BR requires more transmissions than PRR×d in all scenarios except scenario 2 where BR performs better. Given that r is similar for BR and PRR×d, the difference in the energy efficiency is determined by the number of transmissions. BR consumes between 2 to 25% more energy than PRR×d, only in scenario-2 performed 4% worse. On the other hand, in the two scenarios where scenarios where Greedy has a non-zero r, it consumed 3% and 54% more energy than PRR×d. It is interesting to observe that the energy "wasted" by greedy forwarding depends on where the first weak link is encountered. In some scenarios the first weak link is at the beginning of the chain and hence the energy wasted is not significant, however, in other scenarios the weak link is present at the middle or end of the chain which caused a greater energy waste.

Although this experimental study is limited in size, it provides two important conclusions. First, it does serve to confirm and validate our earlier findings from the analytical and simulation studies regarding the PRR×d metric. And second, it shows that the best reception metric is also a good metric for real deployments. Based on the insights of section 6, we believe that higher densities will lead to bigger savings in terms of energy for the PRR×d metric with respect to other strategies.

9. CONCLUSIONS AND FUTURE DIRECTIONS

We have presented a detailed study of geographic routing in the context of lossy wireless sensor networks. Using a realistic link loss model, we have provided a mathematical analysis of the optimal forwarding distance for both ARQ and No-ARQ scenarios, as well as a detailed simulation study in which we proposed and evaluated several novel blacklisting and neighbor selection geographic forwarding strategies. We have also validated some of our approaches using experiments on motes.

Although, the results shown here are for a specific model; the framework, strategies and conclusions are quite robust and can be applied to other models as well. As a matter of fact, an earlier version of this paper used a channel model based on [Woo et al. 2003], which is less accurate than the current model. Even though the earlier model has a more uniform distribution of packet loss rates, the main results and conclusions observed are consistent between the two models.

Key results from our study indicate that the common greedy forwarding approach would result in very poor packet delivery rate. Efficient geographic forwarding strategies do take advantage of links in the high variance transitional region both for energy-efficiency and to minimize route disconnections. An important forwarding metric that arose from our analysis, simulations and experiments is PRR×d, particularly in high-density networks where ARQ is employed. Our results show that reception-based forwarding strategies are generally more efficient than distance-based strategies. We also show that ARQ schemes become more important as the network gets larger. We also compared our local metric to the global optimum and have shown that it remains within a constant value at different densities and network sizes due to the spatial locality of low power wireless graphs.

The PRR×d metric is recommended for static or low dynamic environments, such as environmental monitoring. In highly dynamic environments the link quality can change drastically throughout time and stable estimates of PRR may not be

possible. We hope to develop suitable metrics for such dynamic scenarios in our future work.

Finally, it is important to recall that the scope of this work is on low-rate/time scheduled applications. In these applications interference is not significantly present, however, for scenarios with medium and high traffic rates interference is a necessary characteristic to take into account, and will be considered as part of our future work.

REFERENCES

BOSE, P., MORIN, P., STOJMENOVIĆ, I., AND URRUTIA, J. 2001. Routing with Guaranteed Delivery in Ad Hoc Wireless Networks. *Wireless Networks 7,* 6, 609–616.

BOTTOMLEY, G., OTTOSSON, T., AND WANG, Y. 2000. A generalized RAKE receiver for interference suppression. *Selected Areas in Communications, IEEE Journal on 18,* 8, 1536–1545.

CERPA, A., BUSEK, N., AND ESTRIN, D. 2003. SCALE: A tool for Simple Connectivity Assessment in Lossy Environments. *CENS, UCLA, Tech. Rep.*

CERPA, A., WONG, J., POTKONJAK, M., AND ESTRIN, D. 2005. Temporal properties of low power wireless links: modeling and implications on multi-hop routing. *Proceedings of the 6th ACM international symposium on Mobile ad hoc networking and computing*, 414–425.

CHEN, S., MITRA, U., AND KRISHNAMACHARI, B. 2005. Cooperative communication and routing over fading channels in wireless sensor networks. *Wireless Networks, Communications and Mobile Computing, 2005 International Conference on 2.*

CHUAH, C., TSE, D., KAHN, J., AND VALENZUELA, R. 2002. Capacity scaling in MIMO wireless systems under correlated fading. *Information Theory, IEEE Transactions on 48,* 3, 637–650.

DE COUTO, D., AGUAYO, D., BICKET, J., AND MORRIS, R. 2005. A high-throughput path metric for multi-hop wireless routing. *Wireless Networks 11,* 4, 419–434.

DRAVES, R., PADHYE, J., AND ZILL, B. 2004. Comparison of routing metrics for static multi-hop wireless networks. In *SIGCOMM '04: Proceedings of the 2004 conference on Applications, technologies, architectures, and protocols for computer communications.* ACM, New York, NY, USA, 133–144.

FINN, G. 1987. Routing and Addressing Problems in Large: Metropolitan-scale Internetworks.

FOSCHINI, G. 1996. Wireless Communication in a Fading Environment When Using Multi-Element Antennas. *Bell Labs Technical Journal*, 41.

GANESAN, D., KRISHNAMACHARI, B., WOO, A., CULLER, D., ESTRIN, D., AND WICKER, S. 2003. Complex behavior at scale: An experimental study of low-power wireless sensor networks. *UCLA Computer Science Technical Report UCLA/CSD-TR*, 02–0013.

KARP, B. AND KUNG, H. 2000. *GPSR: greedy perimeter stateless routing for wireless networks.* ACM Press New York, NY, USA.

KHANDANI, A. 2004. Cooperative Routing in Wireless Networks. Ph.D. thesis, Massachusetts Institute of Technology, Dept. of Electrical Engineering and Computer Science.

KIM, Y., GOVINDAN, R., KARP, B., AND SHENKER, S. 2005. Geographic Routing Made Practical. *Proceedings of the USENIX Symposium on Networked Systems Design and Implementation.*

KOTZ, D., NEWPORT, C., AND ELLIOTT, C. 2003. The mistaken axioms of wireless-network research. *Computer Science, Dartmouth College, Technical Report TR2003-467, July.*

KUHN, F., WATTENHOFER, R., AND ZOLLINGER, A. 2003. Worst-Case optimal and average-case efficient geometric ad-hoc routing. *Proceedings of the 4th ACM international symposium on Mobile ad hoc networking & computing*, 267–278.

LEE, S., BHATTACHARJEE, B., AND BANERJEE, S. 2005. Efficient geographic routing in multihop wireless networks. In *MobiHoc '05: Proceedings of the 6th ACM international symposium on Mobile ad hoc networking and computing.* ACM, New York, NY, USA, 230–241.

LI, C., HSU, W., KRISHNAMACHARI, B., AND HELMY, A. 2005. A local metric for geographic routing with power control in wireless networks. *Sensor and Ad Hoc Communications and Networks, 2005. IEEE SECON 2005. 2005 Second Annual IEEE Communications Society Conference on*, 229–239.

LIU, H. AND LI, K. 1999. A decorrelating RAKE receiver for CDMA communications overfrequency-selective fading channels. *Communications, IEEE Transactions on 47,* 7, 1036–1045.

MARCO ZÚ N. Z. AND KRISHNAMACHARI, B. 2007. An analysis of unreliability and asymmetry in low-power wireless links. *ACM Trans. Sen. Netw. 3,* 2, 7.

MAUVE, M., WIDMER, J., AND HARTENSTEIN, H. 2001. A survey on position-based routing in mobile ad hoc networks.

NIKOOKAR, H. AND HASHEMI, H. 1993. Statistical modeling of signal amplitude fading of indoor radiopropagation channels. *Universal Personal Communications, 1993.'Personal Communications: Gateway to the 21st Century'. Conference Record., 2nd International Conference on 1.*

RAPPAPORT, T. 2002. *Wireless communications.* Prentice Hall PTR Upper Saddle River, NJ.

SEADA, K. AND HELMY, A. 2005. Geographic Protocols in Sensor Networks. *Encyclopedia of Sensors, American Scientific Publishers (ASP).*

SEADA, K., HELMY, A., AND GOVINDAN, R. 2004. On the effect of localization errors on geographic face routing in sensor networks. In *IPSN '04: Proceedings of the third international symposium on Information processing in sensor networks.* ACM, New York, NY, USA, 71–80.

SEADA, K., ZUNIGA, M., HELMY, A., AND KRISHNAMACHARI, B. 2004. Energy-efficient forwarding strategies for geographic routing in lossy wireless sensor networks. *Proceedings of the 2nd international conference on Embedded networked sensor systems*, 108–121.

SEIDEL, S. Y. AND RAPPAPORT, T. S. 914 MHz Path Loss Prediction Model for Indoor Wireless Communication in Multi floored Buildings.

SILVA, F., HEIDEMANN, J., AND GOVINDAN, R. 2003. Network Routing API 9.1.

SZEWCZYK, R., OSTERWEIL, E., POLASTRE, J., HAMILTON, M., MAINWARING, A., AND ESTRIN, D. 2004. Habitat monitoring with sensor networks. *Commun. ACM 47,* 6, 34–40.

WOO, A., TONG, T., AND CULLER, D. 2003. Taming the underlying challenges of reliable multi-hop routing in sensor networks. *Proceedings of the 1st international conference on Embedded networked sensor systems*, 14–27.

ZHANG, H., ARORA, A., AND SINHA, P. Learn on the Fly: Quiescent Routing in Sensor Network Backbones. Tech. rep., Technical Report OSU-CISRC-7/05-TR48, The Ohio State University, 2005.

ZHAO, J. AND GOVINDAN, R. 2003. Understanding packet delivery performance in dense wireless sensor networks. *Proceedings of the first international conference on Embedded networked sensor systems*, 1–13.

ZHOU, G., HE, T., KRISHNAMURTHY, S., AND STANKOVIC, J. 2006. Models and solutions for radio irregularity in wireless sensor networks. *ACM Transactions on Sensor Networks (TOSN) 2,* 2, 221–262.

ZUNIGA, M. AND KRISHNAMACHARI, B. 2004. Analyzing the transitional region in low power wireless links. *Sensor and Ad Hoc Communications and Networks, 2004. IEEE SECON 2004. 2004 First Annual IEEE Communications Society Conference on*, 517–526.